doi:10.3788/gzxb20184705.0516005

不同光功率激励下石墨烯的太赫兹波吸收特性

张文涛[1,2],李赣[1,2],占平平[1,2],李跃文[1,2],张玉婷[1,2]
(1 桂林电子科技大学 电子工程与自动化学院,广西 桂林 541004)
(2 广西光电信息处理重点实验室,广西 桂林 541004)

摘 要:基于太赫兹时域光谱系统和德鲁德模型,测量并分析了少层石墨烯在 600 nm CW 红光和两种衬底下的透过率及电导率.结果发现,高阻硅衬底的石墨烯样品在光场激励下对太赫兹信号的吸收显著增强,而 PET(Polyethylene terephthalate)衬底的石墨烯样品在光场激励下对太赫兹信号的吸收则有微弱减少.相较于无激励光场条件,在 0.5 THz 处,高阻硅衬底石墨烯的电导率提升了 7 倍,PET 衬底石墨烯的电导率下降了 23%.同时实验也验证了在太赫兹波段少层石墨烯的电导为各层石墨烯电导的线性叠加.

关键词:太赫兹;石墨烯;光电导;光场激励;光谱分析
中图分类号:O433.4 **文献标识码**:A **文章编号**:1004-4213(2018)05-0516005-10

Characterizing the Absorption of Terahertz Wave by Graphene under the Excitation of Different Luminous Power

ZHANG Wen-tao[1,2], LI Gan[1,2], ZHAN Ping-ping[1,2], LI Yue-wen[1,2], ZHANG Yu-ting[1,2]
(1 *Institute of Electrical Engineering and Automation, Guilin University of Electronic Technology, Guilin, Guangxi* 541004, *China*)
(2 *Key Laboratory of Optoelectronic Information Processing of Guangxi, Guilin, Guangxi* 541004, *China*)

Abstract: The transmissivity and conductivity of the few-layer graphene with 600 nm CW laser and two substrates are measured and analyzed, based on terahertz time-domain spectroscopy and the Drude model. In this study, the absorption of terahertz signal is obviously enhanced through the graphene on high-resistivity silicon or the absorption of terahertz signal is slightly decreased through the graphene on PET (Polyethylene terephthalate) with the excitation of external laser. At 0.5 THz, the conductivity of the graphene on high-resistivity silicon is increased by 7 times or the conductivity of the graphene on PET is felled to 77%, compared to that without external laser. Meanwhile the experiments verify that the conductance in the few-layer graphene appears as the linear superposition of per layer among the THz waveband.

Key words: Terahertz; Graphene; Photoconduction; Laser excitation; Spectroscopy analysis
OCIS Codes: 160.4236; 040.2235; 300.6495; 260.5150

0 Introduction

Terahertz (THz) technology is hailed as one of the ten leading-edge technologies to change the world. In recent years, many problems in the THz devices were solved and the stable techniques of emission and detection of THz have been developed due to the rapid development of ultrafast electronics,

Foundation item: The National Natural Science Foundation of China (No.61565004), Scientific Research and Technological Development Project of Guilin (No.20150133-3)
First author: ZHANG Wen-tao (1976—) male ,professor, Ph.D. degree, mainly focuses on photoelectric detection. Email:glietzwt@163.com
Received: Dec.20, 2017; **Accepted**: Feb.7, 2018

microelectronics, and laser technology[1-2]. Among these techniques, the THz Time-Domain Spectroscopy (THz-TDS)[3] can record not only the amplitude but also the phase information of THz signals. The THz-TDS can be also used to obtain other parameters of samples (e.g., transmissivity, absorption coefficient, and electrical conductivity), which are independent on the K-K relations (Kramers-Kronig relations). Therefore, the THz-TDS has led to a new epoch of developing the THz technology. The THz wave has many excellent properties. For example, the THz wave will not cause damage inside samples because of its extremely low photon energy. In addition, the THz can pass through the nonpolar carriers like pottery, porcelain, and plastic easily[4-5]. Wallace et al.[6] use terahertz pulsed imaging to distinguish cancerous tissue from normal tissue and it could be used to remove the edge of tumor preoperatively. Nie et al.[7] use the THz-TDS to identify transgenic and non-gmo soybeans accurately. Finally, the THz wave has broad applications in the security examination, material testing, radio communication, and so on[8-10].

The excellent properties of the tunable energy gap, ultrahigh carrier mobility and plasma frequency in the THz frequency band make graphene have great potential in the development of a new generation of high-performance THz devices, which will promote development of the high speed THz technology at room temperature[11-12]. In recent years, the output power of the THz quantum cascade laser (THz-QCL) achieves milliwatt in a wide range of frequency (0.68～4.9 THz), but it cannot be operated at room temperature[13]. In contrast, with the strong interaction between graphene and optical phonon, population inversion is induced and THz wave is obtained. It is expected to increase the output power of THz wave to milliwatt at room temperature by electron injection[14]. In addition, THz devices such as schottky diode, field effect transistor have problems with low detection frequency or low response rate. Graphene with ultrahigh carrier mobility can effectively solve such problems. Previous theoretical studies have shown that absorptivity of photons for the single-layer graphene is about 2.3%, and such an absorptivity is wavelength-independent[15]. However, the absorptivity of graphene is slightly higher than the theoretical value in measurements, which is due to the influence of preparation process and environmental factors. In recent years, increasing the THz absorptivity of graphene to achieve a higher modulation depth is the development trend of graphene THz devices. Sensale-Rodriguez et al. demonstrate an effective way to achieve a graphene-based electro-absorption modulator with an extraordinary modulation depth ～64% by concentrating the electric field intensity in an active layer of graphene[16]. Furthermore, Ahmadivand et al. achieve a maximum absorptivity ～67% by combining graphene with plasma metamaterials[17]. In addition, Zou et al. design an arm-type metal mesh structure, which makes graphene modulation depth～28.2% for terahertz signals[18].

In this paper, the transmissivity of graphene with the PET and high-resistivity silicon substrates are measured by using THz-TDS. And, the variations of the THz conductivity and transmissivity of graphene are analyzed under the excitation of laser field. The results show that the Fermi level and carrier concentration of graphene are effectively controlled by light excitation which is a more direct and convenient modulation method than other's. Additionally, in graphene devices, the interaction between the graphene extension and substrate can make graphene's internal electronic state change, therefore, different band widths of graphene materials can be obtained by switching the type of substrates or the number of graphene layers[19]. The purpose of this paper is to explore the influences of substrate material and excitation of laser field on the THz transmissivity and conductivity of graphene by conducting experiments and theoretical calculations. These experimental and theoretical studies can help develop the modulation device of THz signals.

1 Experiments

1.1 Experimental apparatus

In this paper, a transmission-type THz-TDS, which is shown in Fig.1, was used. The pulse emitted by a femtosecond laser is split in two by a beam splitter, and one of the more powerful pulses is used as a pump light to excite a THz wave through the GaAs photoconductive antenna. Such a THz wave passes through the sample by collimating and focusing. Then the THz wave with the information of the sample hits the photoelectric crystal of zinc telluride. As a probe beam, the second pulse passes through the

photoelectric crystal of zinc telluride and finally is received by the photoelectric differential detector[20]. The polarization of the probe beam passing through the crystal will be changed considering the fact that the photoelectric crystal of zinc telluride switches immediately from isotropy to anisotropy under the irradiation of THz beam. Once the transformation of polarizing character is received by the photoelectric differential detector, the time-domain signal of THz wave can be detected after the phase-locking amplifier amplifies the signal and input it into a computer. In order to prevent absorbing too much THz wave by water molecules, some parts of the device are placed in a sealed box with the humidity below 4% by crushing the dry air by a compressor.

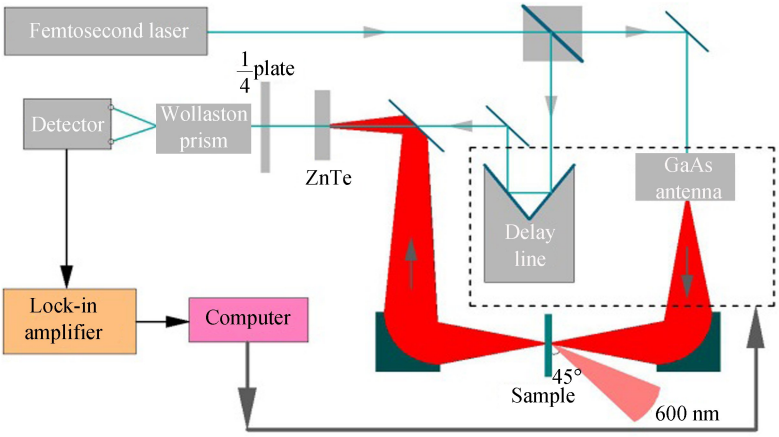

Fig.1 The schematic diagram of THz-TDS system

In this paper, we select 600 nm Continuous Wave (CW) laser with a practical luminous power ~130 mW as an excitation laser field. Such light is radiated to the surface of graphene with an angle of 45° shown in Fig. 1. In the experiment, 70% and 30% filters are placed vertically on the excitation path respectively so that four luminous power gradients (i.e., 0 mW, 39 mW, 87 mW and 130 mW) can be obtained.

1.2 Sample preparation

In this paper, we select two different materials (i.e., PET and high-resistivity silicon), which have high and stable transmissivity in the THz frequency domain, as graphene's substrates. The graphene samples used in this paper are transferred from the copper base by the PMMA (Polymethyl Methacrylate) auxiliary transfer method. The first step is to smear a layer of PMMA film on the surface of copper foil with naturally growing graphene. The second step is that we put the system into $FeCl_3$ solution to corrode the copper foil and then clean the system with the deionized water (DI). Finally, we remove PMMA with acetone on the target material. The samples of graphene at different layers (1, 3, 5 layers) can be obtained by repeating the above transfer steps. The single layer of graphene naturally grows on the copper foil by the traditional CVD method[21], and multiple (20~40) layers of graphene can be obtained in CVD method by replacing the copper foil with the nickel foil.

1.3 Data acquisition

Based on the sample preparation described above, we select the graphene on the PET and high-resistivity silicon substrates to conduct the control experiments. In these experiments, four luminous power gradients (i.e., 0 mW, 39 mW, 87 mW, 130 mW) are used. In addition, three samples for each of 1, 3, 5, and multiple layers are prepared. Finally, five sets of data are measured for each sample at the same luminous power, and there are totally 480 sets of data are recorded.

2 Results and discussion

2.1 Time-domain spectrum analysis

The 480 sets of data obtained from the experiments are transformed into the THz time-domain spectrogram by preprocessing like unification, smoothing, and averaging.

Fig.2 shows the time domain spectra of samples of single-layer graphene on the PET and high-resistivity silicon substrates with different luminous powers of excitation lase field.

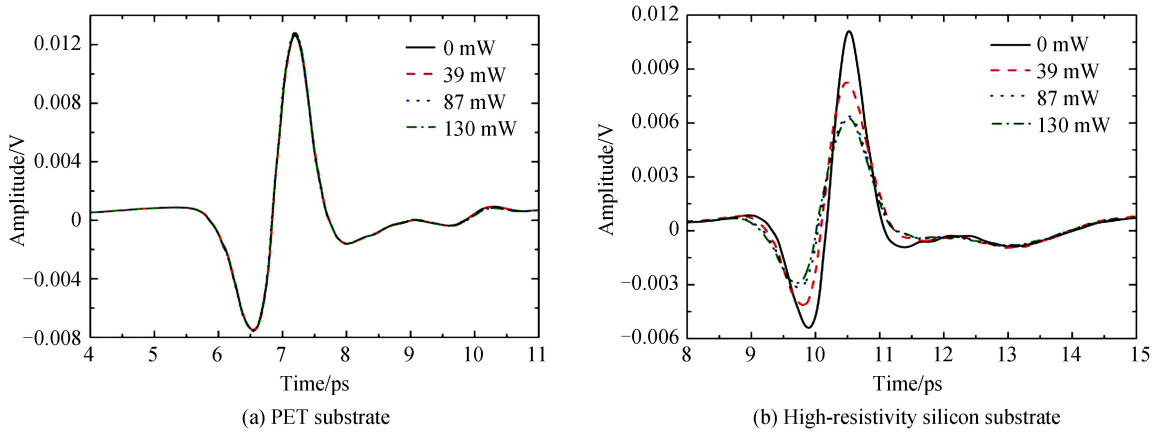

Fig.2 The THz time-domain waveform of single-layer graphene sample

In Fig.2, the THz signal of the graphene sample on the PET substrate does not change significantly by the modulation of the excitation laser field, nevertheless. On the other hand, the THz signal on thehigh-resistivity silicon substrate significantly reduces by the increase of excitation luminous power. By comparing the value of primary signal peak under the excitation of the luminous power at 130 mW and the value without the excitation, we can find that the attenuation of primary signal peak is 43.8%, 42.1%, 39.7%, and 14.9% for 1, 3, 5 and n layers graphene on the high-resistivity silicon substrate, respectively. Therefore, we conclude that that the influence of the excitation of laser field on grapheme significantly decreases when the number of the layer of graphene increases.

2.2 Transmission spectrum analysis

In order to further analyze the sample data, we conduct the Fast Fourier Transform (FFT) analysis for the THz signals on the two different substrates. Based on the FFT analysis, we obtain the distribution of frequency for the THz signals. The THz signal measured in the experiments can be calculated as follows.

$$E_{\mathrm{ref}}(\omega)=E_{0}(\omega)\exp\left(-\mathrm{i}\frac{n(\omega)\omega l}{c}\right) \tag{1}$$

where ω is the frequency of the THz signal, n is the refractive index and l is the propagation distance in the air. Based on the Fresnel formula, the transmittance of THz signal can be expressed as below when the THz signal passes through the sample vertically.

$$t_{\mathrm{ab}(\omega)}=\frac{2n_{\mathrm{a}}(\omega)}{n_{\mathrm{b}(\omega)}+n_{\mathrm{a}}(\omega)} \tag{2}$$

where n_{a} is the incident refractive index and n_{b} is the refractive index for exit. The Fabry-Perot interference can be neglected due to the thin sample, so the THz signal of the sample with d thickness is calculated as following.

$$E_{\mathrm{trans}}(\omega)=E_{\mathrm{ref}}\exp\left(-\mathrm{i}\frac{n(\omega)\omega d}{c}\right)t_{\mathrm{ab}}(\omega)t_{\mathrm{ba}}(\omega) \tag{3}$$

The complex transmissivity of the sample is shown as below.

$$T(\omega)=\frac{4n(\omega)}{[1+n(\omega)]^{2}}\exp\left\{-\mathrm{i}\frac{[n(\omega)-1]\omega d}{c}\right\} \tag{4}$$

The above formula is also the base for extracting optical parameters of samples[22]. Considering that the calculation need to eliminate the influence of blank substrate, the THz signal through the blank substrate is selected as reference signal in this paper. The relative transmissivity of samples can be calculated as below.

$$T'(\omega)=\left[\frac{A_{\mathrm{tran}}(\omega)}{A'_{\mathrm{ref}}(\omega)}\right]^{2} \tag{5}$$

where $A_{\mathrm{trans}}(\omega)$ is the amplitude of THz signal through graphene sample, $A'_{\mathrm{ref}}(\omega)$ is the amplitude of THz signal through blank sample. Combined with Eq.(4), the relationship between transmissivity and conductivity is obtained

$$\varepsilon(\omega)=\sqrt{\frac{\varepsilon_0}{\mu_0}}\left(\frac{1}{\sqrt{T(\omega)}}-1\right)\left(2+\frac{c\varphi(\omega)}{\omega d}\right) \tag{6}$$

where $\varepsilon_0=\frac{1}{36\pi}\times10^{-9}$ F/m is the permittivity of vacuum, $\mu_0=4\pi\times10^{-7}$ N·A^{-2} is the permeability of vacuum, $\varphi(\omega)$ is the phase difference between the sample and the reference. According to Eq. (5), the transmissivity function of samples under the excitation of different luminous powers is shown in Fig.3 and Fig.4.

Fig.3 shows that the transmissivity of graphene samples on the substrate of high-resistivity silicon, which suggests regular characteristics for the illuminant frequency and excited luminous power. In the absence of excitation light, the few-layer graphene samples have a relatively stable transmissivity in the THz wave. On the other hand, under the excitation of laser field, the transmissivity of graphene sample significantly decreases with the increase of THz frequency. In particular, the absorption peak appears around 1.3 THz. The transmissivity of few-layer graphene also has a strong response to the excitation of luminous power, in which, the lower the transmissivity corresponds the larger power. We know that the band gap of silicon is 1.12 eV and the cutoff wavelength of intrinsic absorption is about 1100 nm. There are plenty of electrons on the substrate are stimulated from valence band to conduction band under the excitation of the laser field at 600 nm, and those stimulated carriers diffuse into the grapheme samples in addition to these carriers inside the samples. Therefore, the conductivity of the graphene samples becomes larger and the absorptivity of THz wave is enhanced. Multi-layer graphene has the same trends in response to luminous power as these for the few-layer graphene, but the response to the luminous power is smaller in the former than the latter.

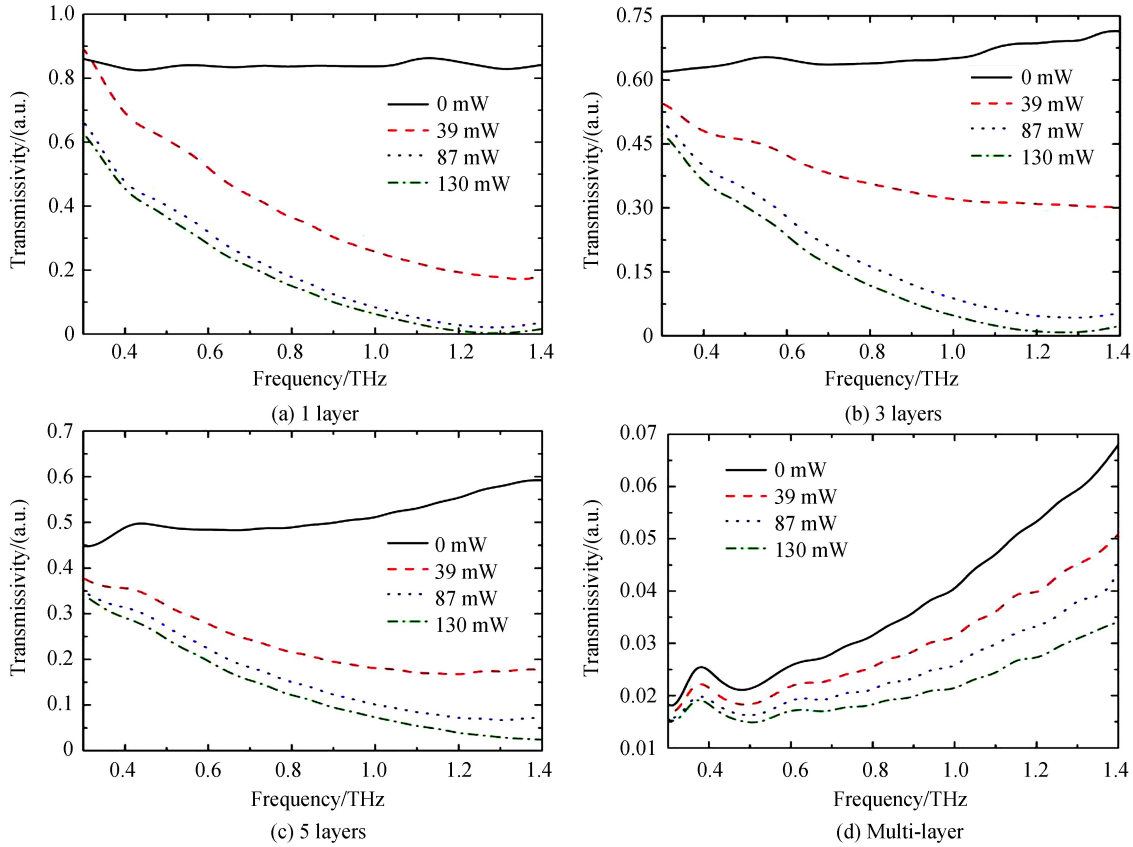

Fig.3 The transmissivity of graphene samples on the substrate of high-resistivity silicon

Fig.4 shows that the transmissivity of PET-graphene is not stable in the range of 0.3～1.4 THz. In particular, the peaks of absorption appear around 0.7 THz, 1.0 THz, and 1.3 THz. The transmissivity of PET-graphene displays an increasing trend with a relatively constant growth rate at each frequency in response to the increase of luminous power. Even under the excitation of luminous power, the conduction

band of PET basically does not have movable electrons because that the PET has a wide band gap and its cutoff wavelength of intrinsic absorption is less than 600 nm. In addition, a large number of electrons in graphene take up high energy levels under the excitation of luminous power. Therefore, the probability of radiation by simulated electrons is less than that of absorption of stimulated electrons and hence population inversion in graphene is induced[23]. Meanwhile, the electrons in graphene undergo stimulated radiation when the THz beam passes through graphene, which amplifies the THz signal. In the wide band of 0.3～1.4 THz, the THz wave increases stably and the average modulation rate is relatively stable too.

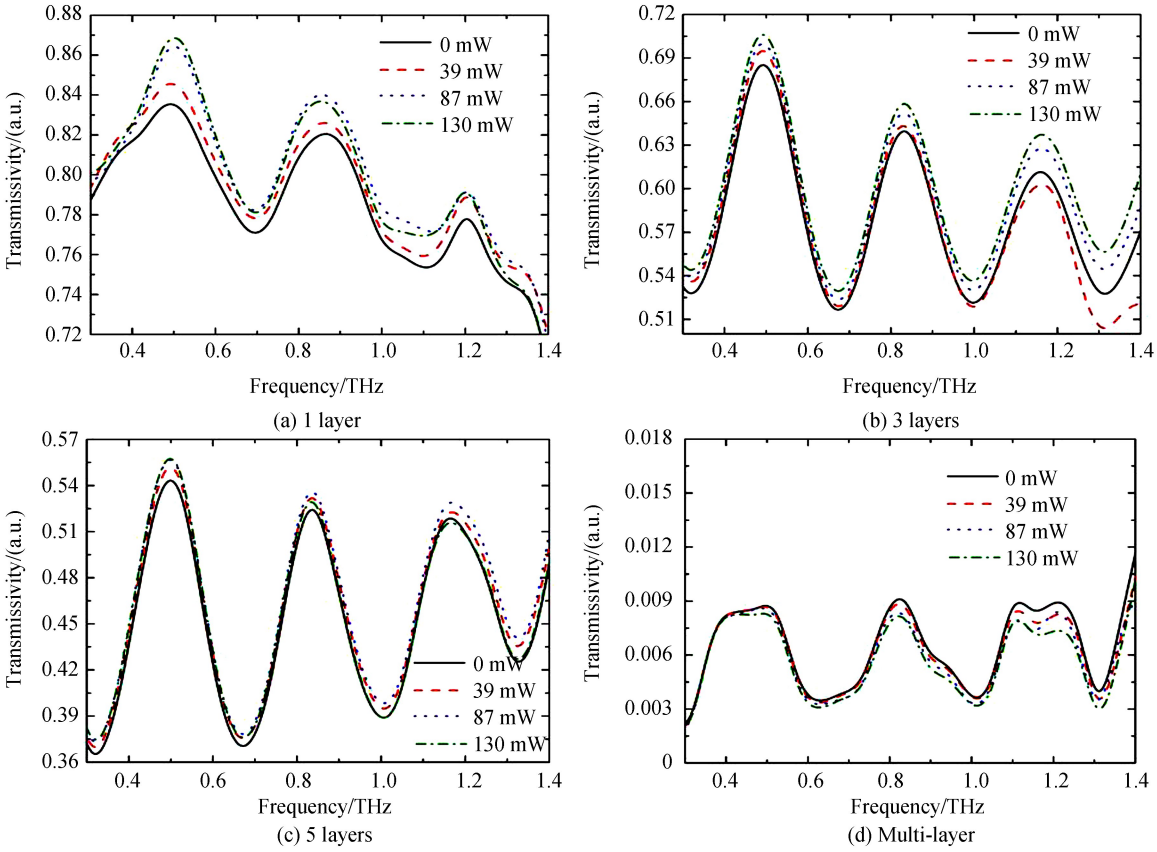

Fig.4 The transmissivity of graphene samples on PET

2.3 Conductance analysis

In order to further discuss the way of modulating the THz signal by graphene, we also calculate the conductance of the THz signal in graphene to explore the effect of the excitation to the photoconductance of graphene. In this section, the characteristics of conductance of the THz signal in the few-layer graphene are discussed based on the hypothesis that the conductance of the THz signal in the few-layer graphene appears as the linear superposition of per layer without electron coupling among different layers proposed by Dr Zhou[24]. Therefore, the conductivity of the THz signal in the thin layer can be calculated as below.

$$\sigma_{\text{total}}=\frac{1+n}{Z_0}\left(\frac{A_{\text{ref}}}{A_{\text{N}}}-1\right) \tag{7}$$

Furthermore, the conductivity of the THz signal in the thin layer follows the Drude model[25].

$$\sigma(\omega)=\frac{(\nu_{\text{F}}e^2/h)\sqrt{\pi|N_{\text{c}}|}}{\pi(\Gamma+\omega^2/\Gamma)} \tag{8}$$

where $\nu_{\text{F}}=1.1\times10^6\ \text{m}\cdot\text{s}^{-1}$ is Fermi velocity, $e=1.60\times10^{-19}\ \text{C}$ is elementary charge, $h=4.14\times10^{-15}\ \text{eV}\cdot\text{S}$ is Planck constant, $\Gamma=100\ \text{cm}^{-1}$ is probability of carrier scattering, and $Z_0=377\Omega$ is impedance in free space, N_{c} is carrier concentration. The Fermi level of graphene is calculated as below.

$$E_{\text{F}}=\pm h\,\nu_{\text{F}}\sqrt{\pi|N_{\text{c}}|} \tag{9}$$

Based on our calculation, the Fermi level of one-layer graphene on PET is approximately 0.175 eV and the Fermi level ofone-layer graphene on high-resistivity silicon is approximately 0.244 eV. This demonstrates

that the graphene is electron-doped with the influence of the two different substrates. We take the THz signal on the blank substrate as a reference when processing data. Based on Eq. (7), we have the conductance of graphene in the thin layer shown in Fig.5 and Fig.6.

The conductivity of graphene on high- resistivity silicon is consistent with the theoretical value when there is no excitation of laser field. The conductivity of graphene under the excitation of laser field enhances significantly, and the enhancement increases with the increasing frequency. In addition, the conductivity of graphene also enhances with the increasing excitation, which indicates that stimulated absorption is stronger than stimulated radiation if the excitation is applied to the graphene on the high- resistivity silicon.

Fig.6 shows opposite of the results suggested to Fig.5. The conductivity of THz signal in the few-layer graphene decreases slightly with the increasing excitation by luminous power. The decreasing conductivity shown in Fig.6 have relatively stable variation in 0.3～1.0 THz, which indicates that stimulated radiation is stronger than stimulated absorption for the graphene on PET under the excitation. Furthermore, the decrease of electron results in the decrease of conductivity.

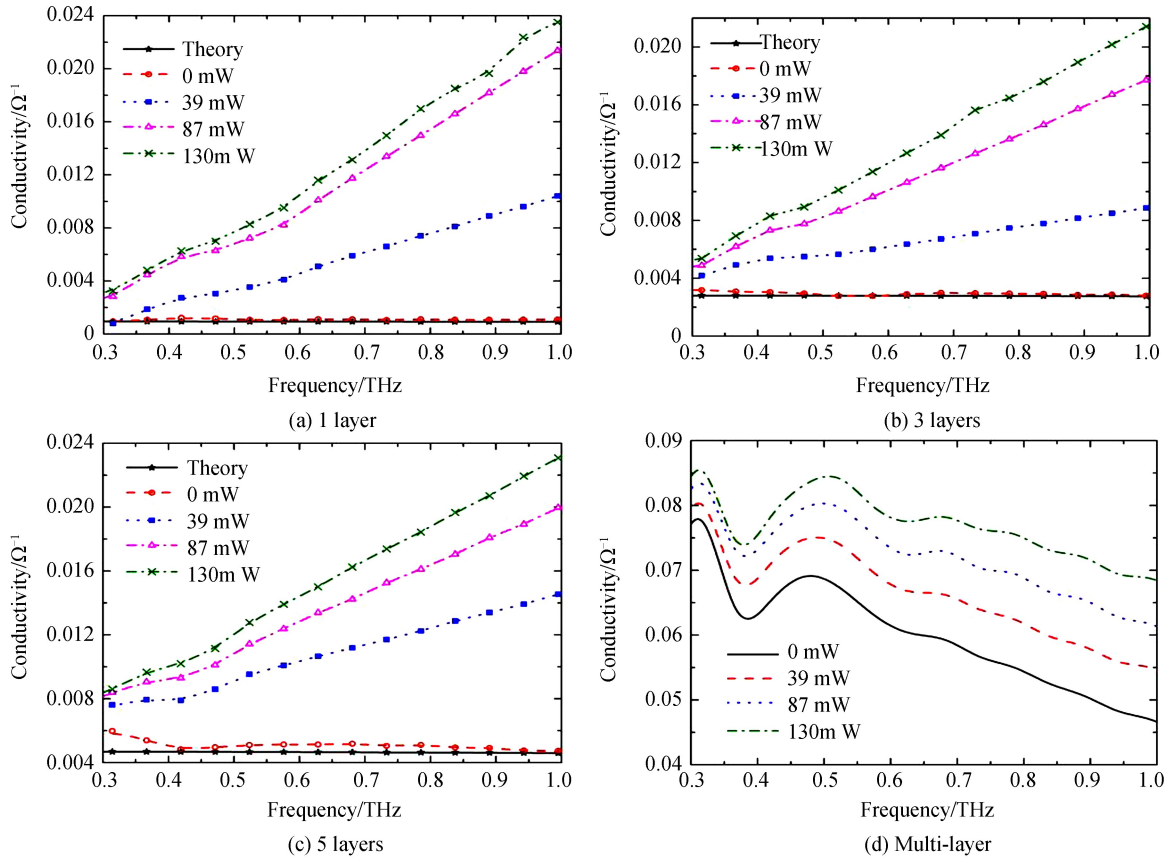

Fig.5 The conductivity of graphene on high- resistivity silicon

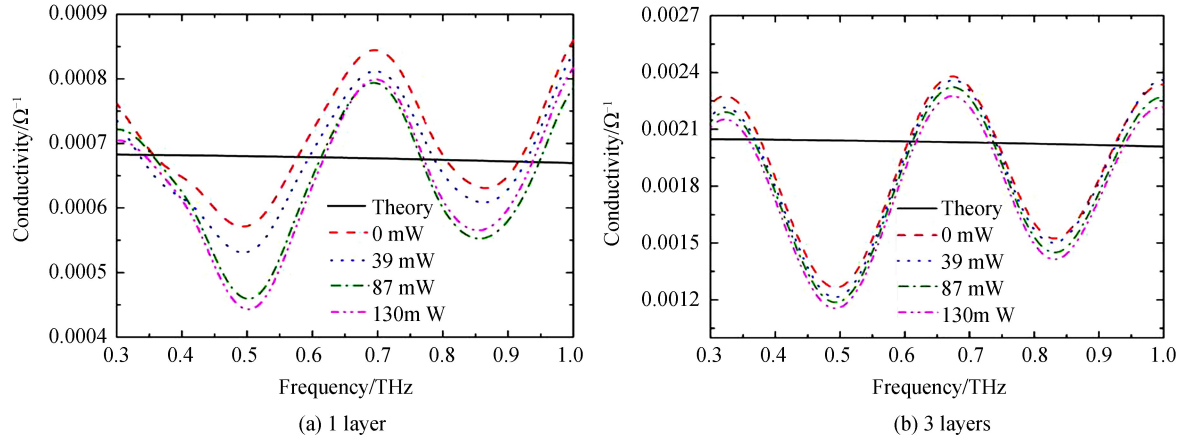

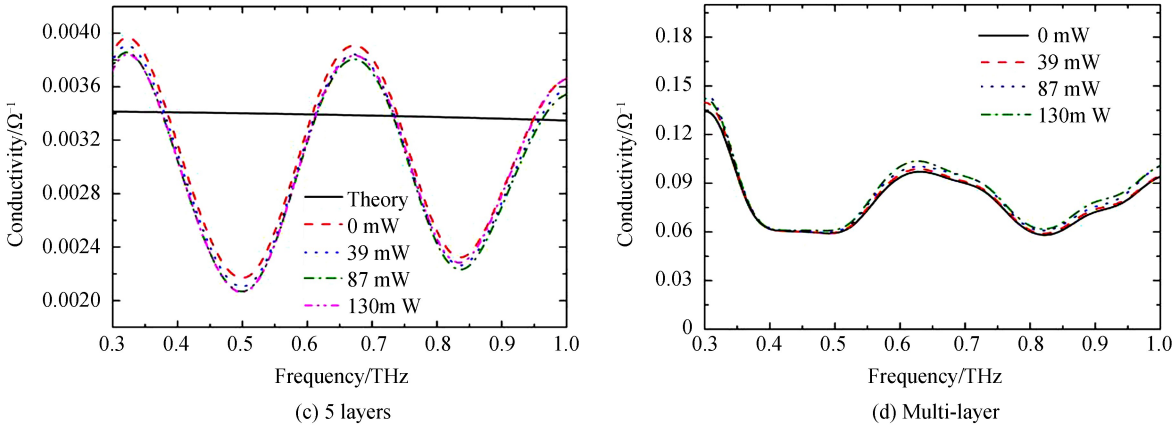

Fig.6 The conductivity of graphene on PET

There is no large difference between the experimental values and the theoretical values for the graphene samples under the two different substrates (i.e., PET and high- resistivity silicon) if there is no excitation of laser field. Within the observation window of 0.3～1.0 THz, the experimental values are basically consistent with the theoretical values.

Fig.7 is a comparison between the theoretical values and the experimental values for the conductivity of the thin-layer graphene without the excitation. Considering that the conductivity of the thin-layer graphene basically keeps a stable value at the frequencies of THz, we average the conductivity of the thin-layer graphene as the experimental value (Fig.7).

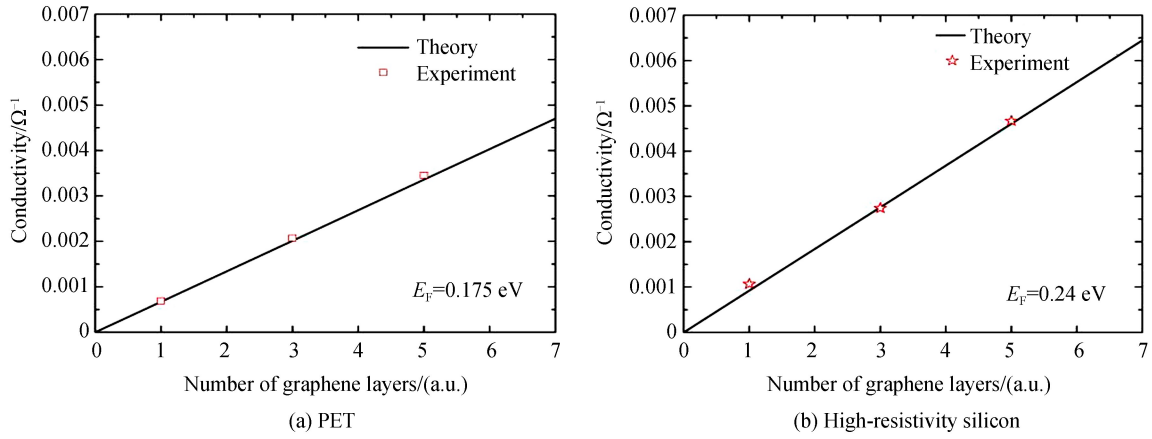

Fig.7 The conductivity of graphene without excitation

The straight lines in Fig.7 are calculated by Eq. (8), which is based on the hypothesis proposed by Dr Zhou[24]. The theoretical results are consistent with the experimental results (circles in Fig.7), which validates the hypothesis by Dr. Zhou. The THz conductivity of graphene can be regarded as the linear superposition of the conductivity of each layer, and the Fermi level is proportional to the slope. In addition, the experimental conductivity of multi-layer graphene (not shown) is much larger than the theoretical value. This is because the hypothesis, in which no electronic coupling exists among different layers, does not hold. The reason why the hypothesis does not hold is because the multi-layers graphene sample is no longer obtained with multiple transfers and the interlamination is no longer random stack.

3 Conclusion

In this paper, we obtain graphene samples with 1, 3, 5, and multiple layers on the two different substrates (i.e., PET andhigh- resistivity silicon) based on the CVD method and PMMA auxiliary transfer method. Under the excitation of 600 nm laser in four gradients (i.e., 0 mW, 39 mW, 87 mW and 130 mW),the THz signals through the samples are measured. In addition, and the variations of the transmissivity and THz conductance are calculated. The graphene samples behave differently with different

substrates under the excitation of laser field, since different substrates can create different band gaps and Fermi levels in the graphene samples. The few-layer graphene samples on the high-resistivity silicon have strong responses to the varying excitation of luminous power and varying THz frequency. Meanwhile, the transmissivity and conductivity of THz are reduced with the increasing luminous power. For the few-layer graphene samples on PET, the transmissivity and conductivity of THz are improved with the enhancing excitation of luminous power. Such a relationship makes it possible for graphene to be amplification gain medium for the THz signals. In future applications, it is expected that graphene THz devices with different modulation functions will be realized by using different substrates. The pump light is just in the range of red, so we also hope to simplify the optical path and realize automatic control by using the pump light of THz as the excitation source of graphene devices. It is clear that graphene has great applications in the THz technology, and our paper provides new ideas for the modulation of THz wave.

References

[1] HU Xiao-yan. Research progress and trends of terahertz technology from the view of photonics[J]. *Laser and Infrared*, 2015, **45**(7): 740-748.

[2] LIU Chao, YANG Ming, LIU Zhi-gang. Development and application in near-terahertz power devices[J]. *Journal of Microwaves*, 2015(s1): 6-9.

[3] DHILLON S S, VITIELLO M S, LINFIELD E H, *et al*. The 2017 terahertz science and technology roadmap[J]. *Journal of Physics D Applied Physics*, 2017, **50**(4): 043001.

[4] YANG Zhen-gang, ZHAO Bi-qiang, LIU Jin-song, *et al*. Nondestructive inspection with terahertz waves[J]. *Physics*, 2013, **42**(10): 708-711

[5] KAWASE K, OGAWA Y, WATANABE Y, *et al*. Non-destructive terahertz imaging of illicit drugs using spectral fingerprints[J]. *Optics Express*, 2003, **11**(20): 2549-2554.

[6] WALLACE V P, FITZGERALD A J, SHANKAR S, *et al*. Terahertz pulsed imaging of basal cell carcinoma ex vivo and in vivo[J]. *British Journal of Dermatology*, 2015, **151**(2): 424-432.

[7] NIE Jun-yang, ZHANG Wen-tao, XIONG Xian-ming, *et al*. Recognition of transgenic soybeans based on terahertz spectroscopy and PCA-BPN network[J]. *Acta Photonica Sinica*, 2016, **45**(5): 161-167.

[8] ZHAO Guo-zhong, SHEN Yan-chun, LIU Ying. Application of terahertz technology in military and security field[J]. *Journal of Electronic Measurement and Instrumentation*, 2015(8): 1097-1101.

[9] SEEDS A J, SHAMS H, FICE M J, *et al*. Terahertz photonics for wireless communications[J]. *Journal of Lightwave Technology*, 2015, **33**(3): 579-587.

[10] HEBLING J, YEH K L, HOFFMANN M C, *et al*. Generation of high-power terahertz pulses by tilted-pulse-front excitation and their application possibilities[J]. *Journal of the Optical Society of America B*, 2015, **25**(7): 1266-1277.

[11] KAN E, REN H, WU F,*et al*. Why the band gap of graphene is tunable on hexagonal boron nitride[J]. *Journal of Physical Chemistry C*, 2012, **116**(4): 3142-3146.

[12] RYZHII V, RYZHII M, MITIN V,*et al*. Terahertz photomixing using plasma resonances in double-graphene layer structures[J]. *Journal of Applied Physics*, 2013, **113**(17): 1308-103.

[13] RENO J L, KHAANAL S, KUNMAR S. 2.1 THz quantum-cascade laser operating up to 144 K based on a scattering-assisted injection design[J].*Optics Express*, 2015, **23**(15): 19689.

[14] SU Juan, CHENG Bin-bin, DENG Xian-jin. Recent progress on graphene-based terahertz optoelectronics [J]. *Information and Electronic Engineering*, 2015, **13**(3): 511-519.

[15] CHEN Ying-liang, FENG Xiao-bo, HOU De-dong. Optical absorptions in monolayer and bilayer graphene[J]. *Acta Physica Sinica*, 2013, **62**(18): 416-421.

[16] SENSALE-RODRIGUEZ B, YAN R, RAFIQUE S, *et al*. Extraordinary control of terahertz beam reflectance in graphene electro-absorption modulators[J]. *Nano Letters*, 2016, **12**(9): 4518-4522.

[17] AHMADIVAND A, SINHA R, KARABIYIK M,*et al*. Tunable THz wave absorption by graphene-assisted plasmonic metasurfaces based on metallic split ring resonators[J]. *Journal of Nanoparticle Research*, 2017, **19**(1): 3.

[18] ZOU Yi-xuan, DONG Lian-he, XIA Liang-ping,*et al*. Graphene electrically modulating terahertz transmission enhanced by arm type metal mesh structure[J]. *Acta Photonica Sinica*, 2018, **47**(2): 0223002.

[19] HABERER D, VVALIKH D V, TAIOLI S, *et al*. Tunable band gap in hydrogenated quasi-free-standing graphene[J]. *Nano Letters*, 2015, **10**(9): 3360-3366.

[20] CHEN Tao, LI Zhi, MO Wei. Identification of terahertz absorption spectra of explosives based on fuzzy pattern recognition[J]. *Chinese Journal of Scientific Instrument*, 2012, **33**(11): 2480-2486.

[21] QI M, REN Z, JIAO Y, *et al*. Hydrogen kinetics on scalable graphene growth by atmospheric pressure chemical vapor deposition with acetylene[J]. *Journal of Physical Chemistry C*, 2013, **117**(27): 14348 - 14353.

[22] DOMEY T D, BARANIUK R G, MITTLEMAN D M. Material parameter estimation with terahertz time-domain

spectroscopy[J]. *Journal of the Optical Society of America A Optics Image Science and Vision*, 2001, **18**(7): 1562-71.

[23] LI T, LUO L, HUOALO M, *et al*. Femtosecond population inversion and stimulated emission of dense Dirac fermions in graphene.[J]. *Physical Review Letters*, 2012, **108**(16): 167401.

[24] ZHOU Yi-xuan, ZHENG Xin-liang, XU Xin-long, *et al*. Study on terahertz conductivity of stacked multilayer graphene [J]. *China Sciencepaper*, 2014(6): 673-676.

[25] MAENG I, LIM S, CHAE S J, *et al*. Gate-controlled nonlinear conductivity of dirac fermion in graphene field-effect transistors measured by terahertz time-domain spectroscopy[J]. *Nano Letters*, 2012, **12**(2): 551.